Electronic Supplementary Material (ESI) for Polymer Chemistry.
This journal is © The Royal Society of Chemistry 2023

Electronic Supplementary Information (ESI)

Amphiphilic tetra-PCL-*b*-PEG star block copolymers using benzoxazinone-based linking groups

Carolin Bunk,[1,2] Hartmut Komber,[1] Michael Lang,[1]* Nora Fribiczer,[3] Martin Geisler,[1] Petr Formanek,[1] Lothar Jakisch,[1] Sebastian Seiffert,[4] Brigitte Voit,[1,2] Frank Böhme[1]*

[1] Leibniz-Institut für Polymerforschung Dresden e. V., Hohe Str. 6, 01069 Dresden, Germany
[2] Organische Chemie der Polymere, Technische Universität Dresden, 01062 Dresden, Germany
[3] Department Chemie, Johannes Gutenberg-Universität Mainz, Duesbergweg 10-14, 55128 Mainz, Germany

Correspondence:
boehme@ipfdd.de
lang@ipfdd.de

Table of Contents

1. Dynamic Light Scattering (DLS)

The amplitude correlation functions $g^{(1)}(q,t)$ received from the DLS experiment for different scattering vectors q are fitted with monoexponential decay functions, $g^{(1)}(q,t) = A\cdot exp\left(\frac{-t}{\tau(q)}\right)$, for all solvents except of acetone. In the latter case, only a biexponential decay $g^{(1)}(q,t) = A\cdot exp\left(\frac{-t}{\tau_1(q)}\right) + B\cdot exp\left(\frac{-t}{\tau_2(q)}\right)$ provided a satisfying agreement with the data, see Figure **S1**. Here, A and B are the amplitudes, t is the time, and the characteristic relaxation times for a particular q are given by $\tau_i(q)$ with i = 1,2. For all samples analyzed, the quality of the data and the fit is comparable to the examples shown in Figure **S1**. The diffusion coefficient D is received as the slope from plotting $\tau_i(q)$ against q^2. The hydrodynamic radii are calculated using the Stokes-Einstein relation $R_H = \frac{k_B T}{6\pi\eta D}$, with the Boltzmann constant k_B, the absolute temperature T, and the dynamic viscosity of the solvent η. Reference values for the dynamic viscosity of the solvents at 20°C were taken from literature and are 0.437, 0.325, 0.452, and 1.003 (all in units of mPa·s) for dichloromethane [1], acetone [2], ethyl acetate [2], and water [3], respectively. Scattering vectors were computed for a given scattering angle using the wave length of 632.8 nm of the laser beam and literature data for the refractive index, which is 1.4244, 1.3588, 1.3723, and 1.3330 for the above solvents, respectively [1, 4, 5].

References for 1. Dynamic Light Scattering

[1] M. Rossberg, W. Lendle, G. Pfleiderer, A. Tögel, T.R. Torkelson, K. K. Beutel, Chloromethanes. *Ullmann's Encyclopedia of Industrial Chemistry.* (2011). https://onlinelibrary.wiley.com/doi/epdf/10.1002/14356007.a06_233.pub3.

[2] Dortmund Data Bank; http://www.ddbst.com/en/EED/PCP/VIS_C4.php

[3] B. González, N. Calvar, E. Gómez, Á. Domínguez, *J. Chem. Thermodyn.* **39**, (2007) 1578-1588

[4] CRC Handbook of Chemistry and Physics, R. C. Weast, CRC Press Inc.,U.S.; 56th Revised edition (1975), ISBN: 978-0878194551

[5] CRC Handbook of Chemistry and Physics, W. M. Haynes (ed.) 94th Edition. CRC Press LLC, Boca Raton: FL 2013-2014, 3-250

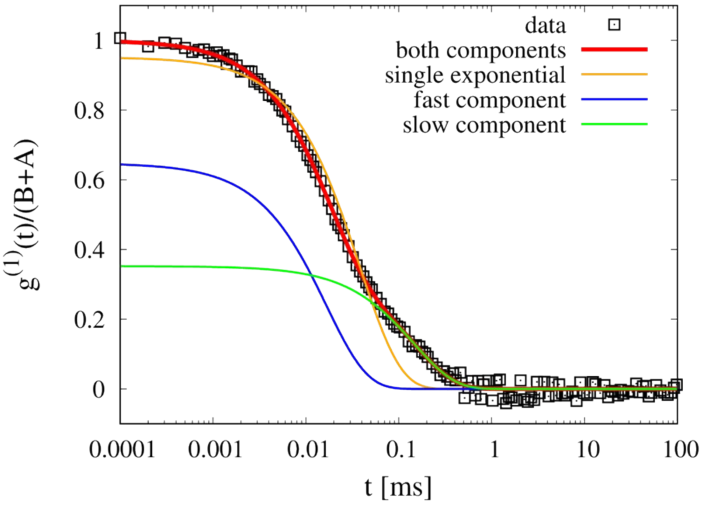

Figure S1. Amplitude correlation function of a 20 g L^{-1} solution of **6b** in acetone. Data were obtained at 90° scattering angle at a temperature of 20 °C and fit by a single and double exponential decay, where for the latter, the contributions of the slow and the fast component are shown.

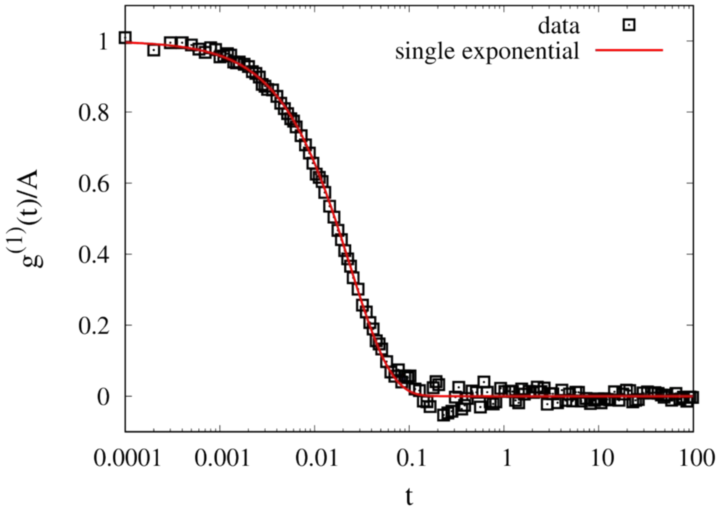

Figure S2. Single exponential decay for 10 g L^{-1} solution of **6b** in ethyl acetate measured at a scattering angle of 90° and a temperature of 20 °C.

Table S1. Hydrodynamic radii of **6a** and **6b** in water and different organic solvents at 20 °C as a function of polymer concentration *c*. *F* is the relative amplitude of the fast component, $F = \frac{B}{A+B}$, in case of a bi-exponential fit. The error margins reflect the error of the numerical data regression. A more detailed discussion of systematic errors and the noise of the data provides no substantially larger errors.

polymer	**solvent**	***c*** (g L^{-1})	***F***	$R_{H,1}$(nm)	$R_{H,2}$(nm)
6b	water	0.025		22.0 ± 0.5	–
		0.05		21.1 ± 0.3	–
		0.1		21.3 ± 0.3	–
		0.25		20.0 ± 0.1	–
		0.5		20.1 ± 0.1	–
		1		19.9 ± 0.2	–
	acetone	2.5	0.76	18.0 ± 1	3.5 ± 0.1
		5	0.69	21.8 ± 0.4	3.6 ± 0.1
		10	0.64	23.8 ± 0.4	3.7 ± 0.1
		20	0.62	34.8 ± 0.9	4.2 ± 0.1
	dichloromethane	10		3.8 ± 0.3	–
	ethyl acetate	5		4.2 ± 0.1	–
		10		4.3 ± 0.1	–
6a	acetone	2.5	0.59	14 ± 1	3.0 ± 0.2
		5	0.55	18.5 ± 0.9	3.2 ± 0.1
		10	0.59	21.5 ± 0.7	3.5 ± 0.1
		20	0.53	23.0 ± 0.4	3.6 ± 0.1

2. NMR spectroscopic investigation of star polymer 1

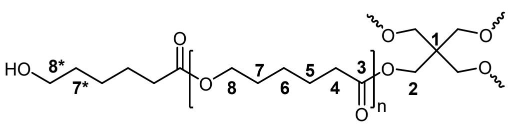

1

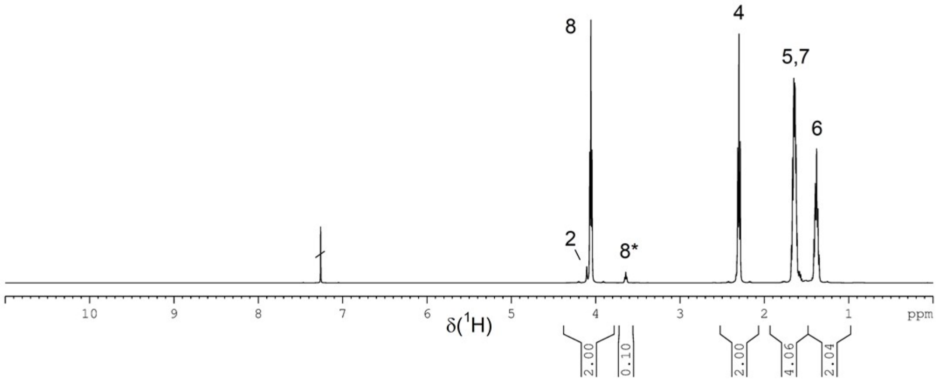

Figure S3. ^{1}H NMR spectrum of **1a** with integral regions used for calculation of the number-average molar mass $M_{n,NMR}$ for **1a** and **1b** as shown in the following comment (solvent: $CDCl_3$).

*Calculation of the molar mass (exemplary for **1a**):*

Average number of PCL units per PCL arm (n):

$n+1 = (0.5 \cdot (I_2 + I_8)) \;/\; (0.5 \cdot I_{8*}) = 1.00 / 0.05 = 20$ (estimated error: ± 2%)

Number-average molecular weight by NMR end group method:

$M_{n,NMR} = 4(n+1) \cdot M_{n,CL} + M_{n,core} = 80 \cdot 114\ \text{g mol}^{-1} + 136\ \text{g mol}^{-1} = 9.300\ \text{g mol}^{-1}$ ($\pm$ 200 g mol^{-1})

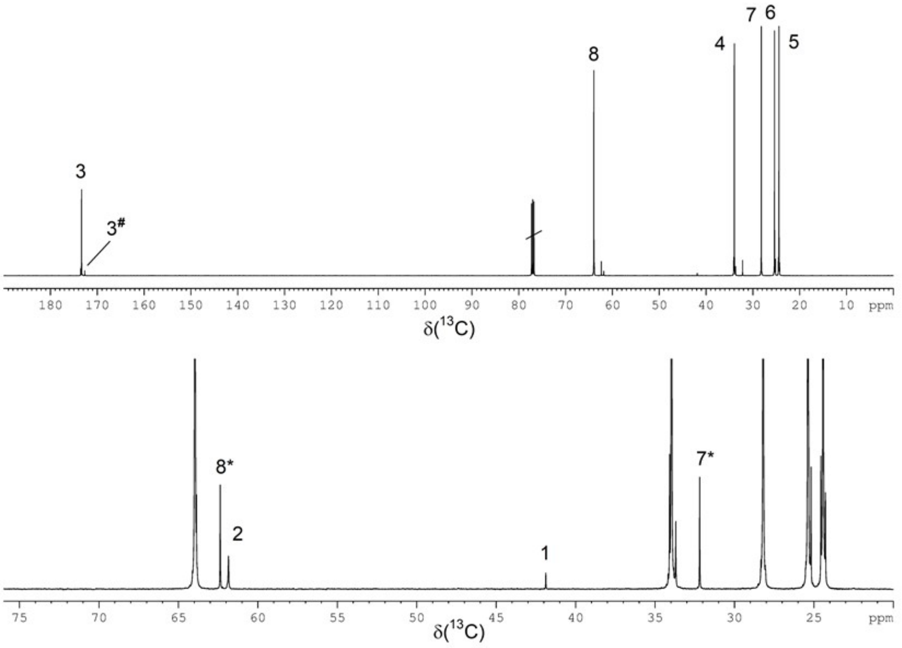

Figure S4. ^{13}C NMR spectrum of **1a** (solvent: $CDCl_3$). $3^{\#}$ is the carbonyl group next to the core.

3. NMR spectroscopic investigation of star polymer 3

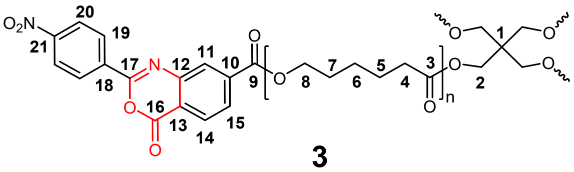

3

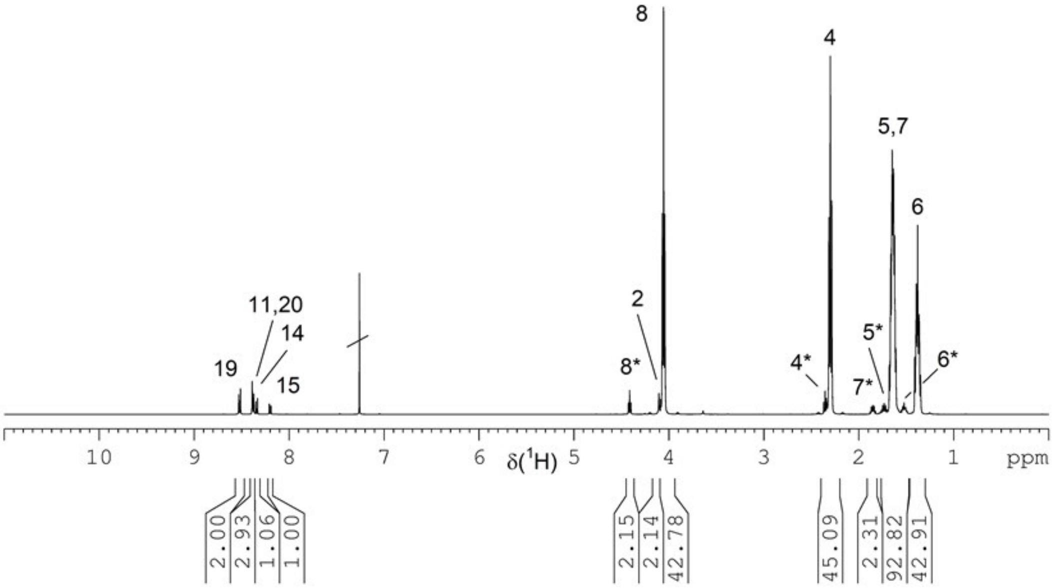

Figure S5. ^{1}H NMR spectrum of **3a** with integral regions used for calculation of the number-average molar mass $M_{n,NMR}$ for **3a** and **3b** as shown in the following comment (solvent: $CDCl_3$). Symbol * indicates that the CL unit is bonded to the terminal oxazinone unit.

*Calculation of the molar mass (exemplary for **3a**):*

Average number of PCL units per PCL arm (n):

$n = 0.5 \cdot (I_2 + I_8)\ /\ (0.5 \cdot I_{8*}) = 22.5 / 1.08 = 21$ (estimated error: ± 2%)

Number-average molecular weight by NMR end group method:

$M_{n,NMR} = 4n \cdot M_{n,CL} + M_{n,core} + 4 \cdot M_{n,BenzOx} = 84 \cdot 114\ \text{g mol}^{-1} + 136\ \text{g mol}^{-1} + 4 \cdot 295\ \text{g mol}^{-1} = 10.900\ \text{g mol}^{-1}$ (± 200 g mol^{-1})

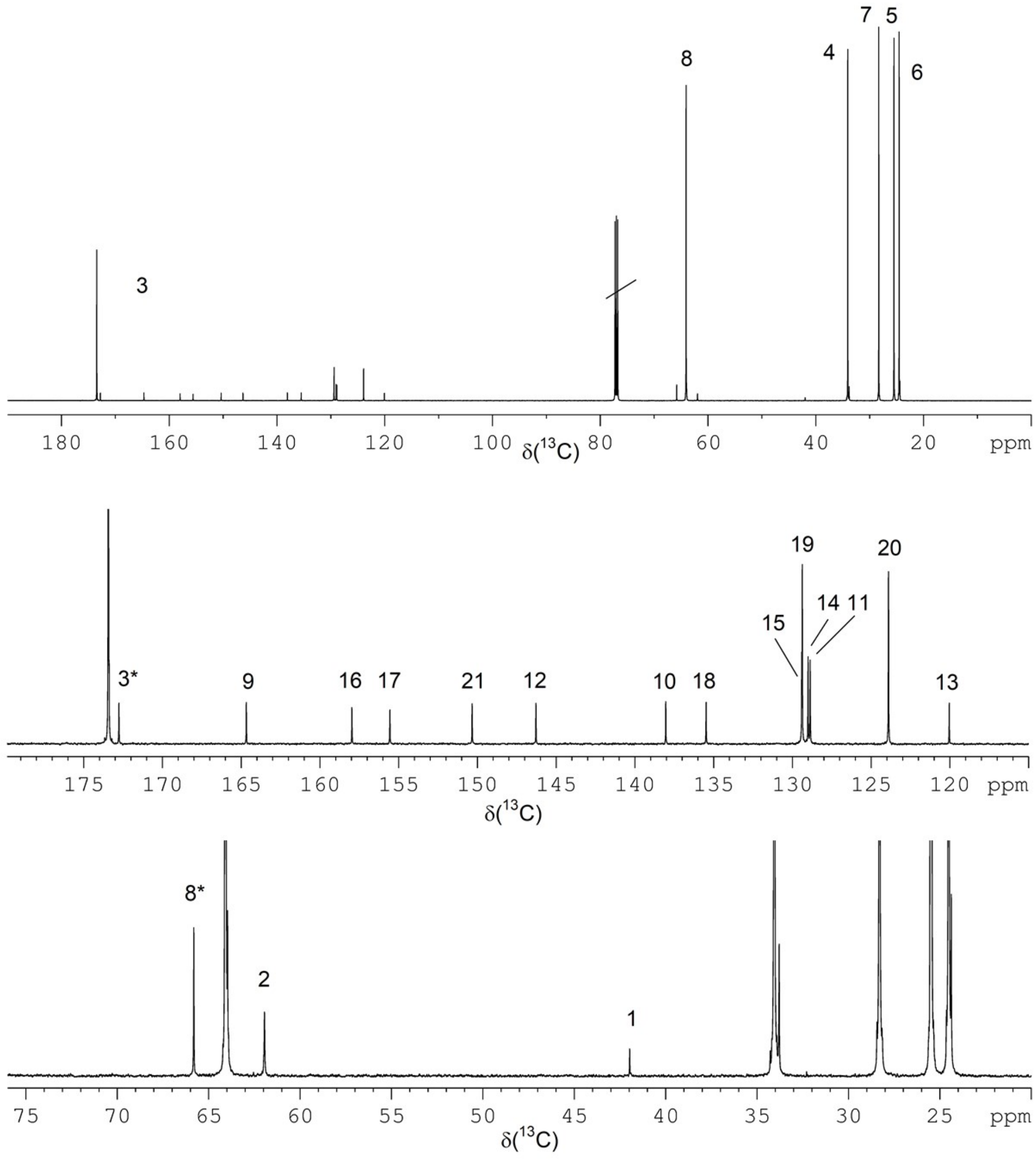

Figure S6. ^{13}C NMR spectrum of **3a** (solvent: $CDCl_3$). Symbol * indicates that the CL unit is bonded to the terminal oxazinone unit.

4. NMR spectroscopic investigation of polymer 5

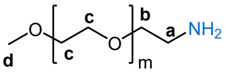

5

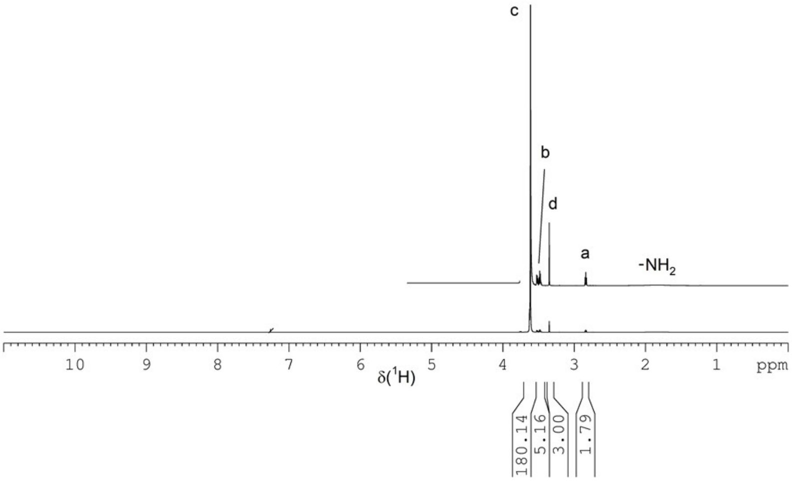

Figure S7. ^{1}H NMR spectrum of **5b** with integral regions used for calculation of the number-average molar mass $M_{n,NMR}$ for **5a** and **5b** as shown in the following comment (solvent: $CDCl_3$).

*Calculation of the molar mass (exemplary for **5b**):*

Number of CH_2CH_2O units (m+1):

$$m + 1 = (0.25 \cdot (I_a + I_b + I_c)) \; / \; (\frac{1}{3} \cdot I_d) = 47$$ (estimated error: ± 2%)

Number-average molecular weight by NMR end group method:

$M_{n,NMR} = m \cdot M_{n,CH2CH2O} + M_{n,CH3O} + M_{n,CH2CH2NH2} = 46 \cdot 44 \text{ g mol}^{-1} + 31 \text{ g mol}^{-1} + 44 \text{ g mol}^{-1} = 2.100 \text{ g mol}^{-1}$ ($\pm$ 100 g mol^{-1})

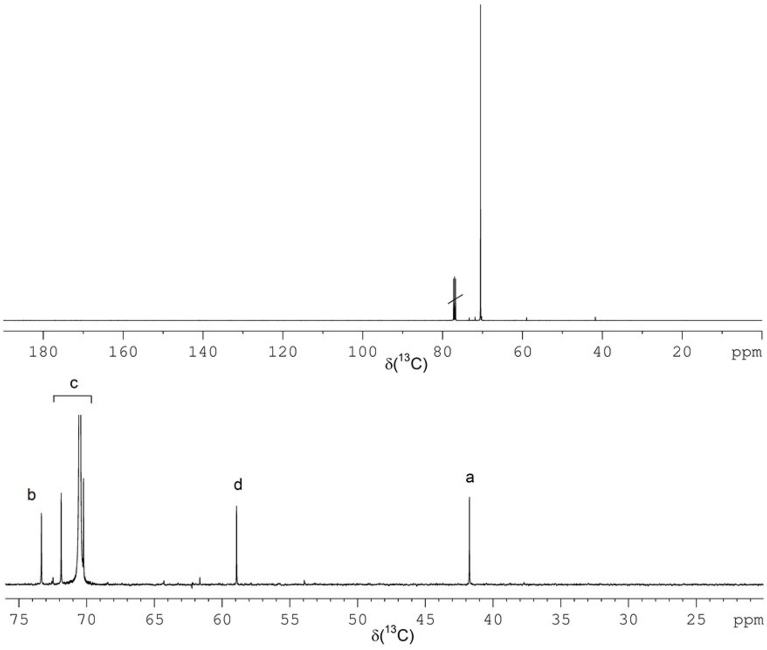

Figure S8. ^{13}C NMR spectrum of **5b** (solvent: $CDCl_3$).

5. NMR spectroscopic investigation of star block copolymer 6

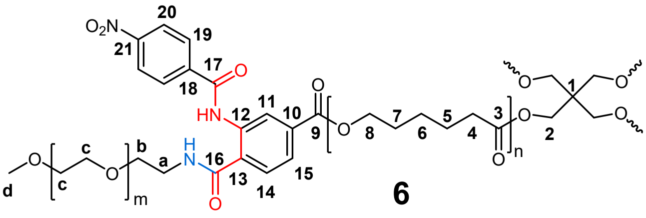

6

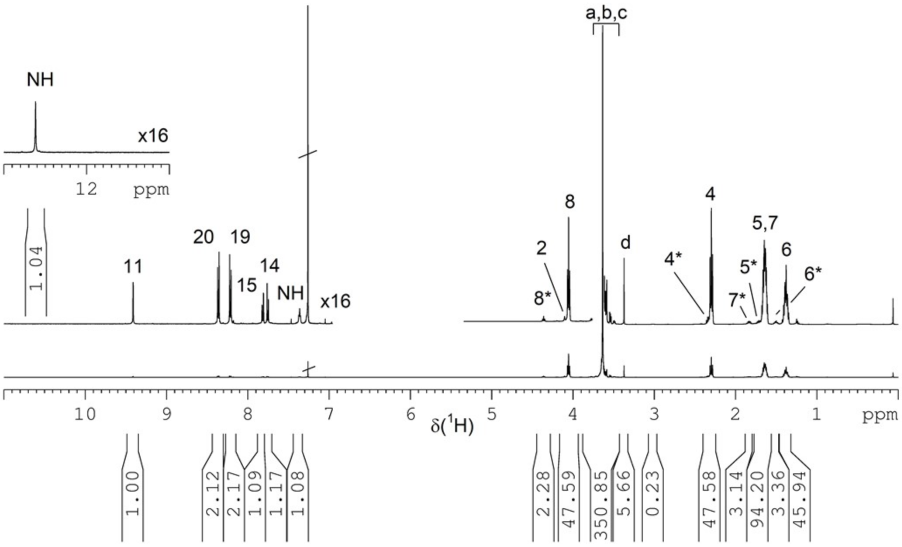

Figure S9. ^{1}H NMR spectrum of **6b** (solvent: $CDCl_3$). * indicates that the CL unit is bonded to the connecting unit.

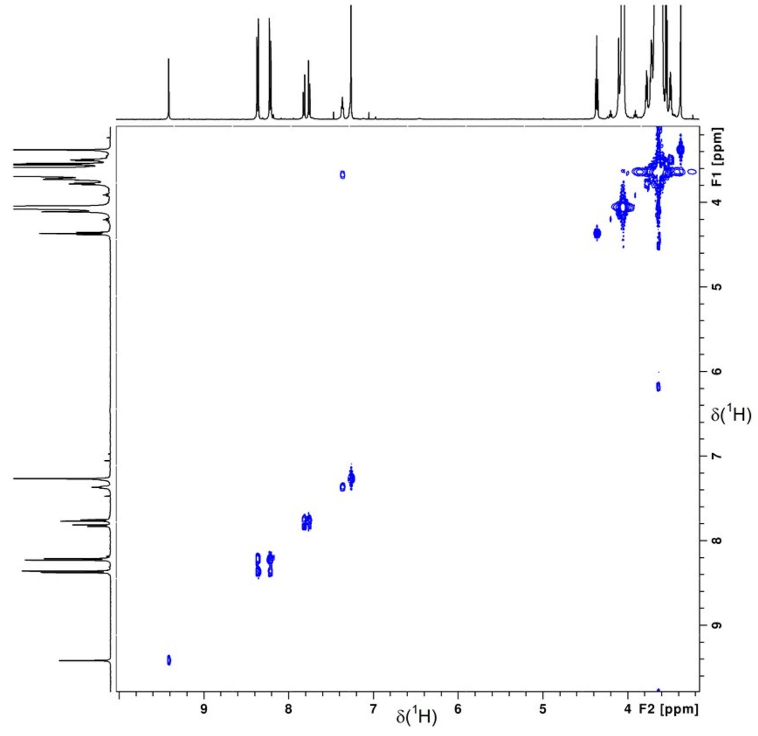

Figure S10. COSY spectrum (region) of **6b** (solvent: $CDCl_3$).

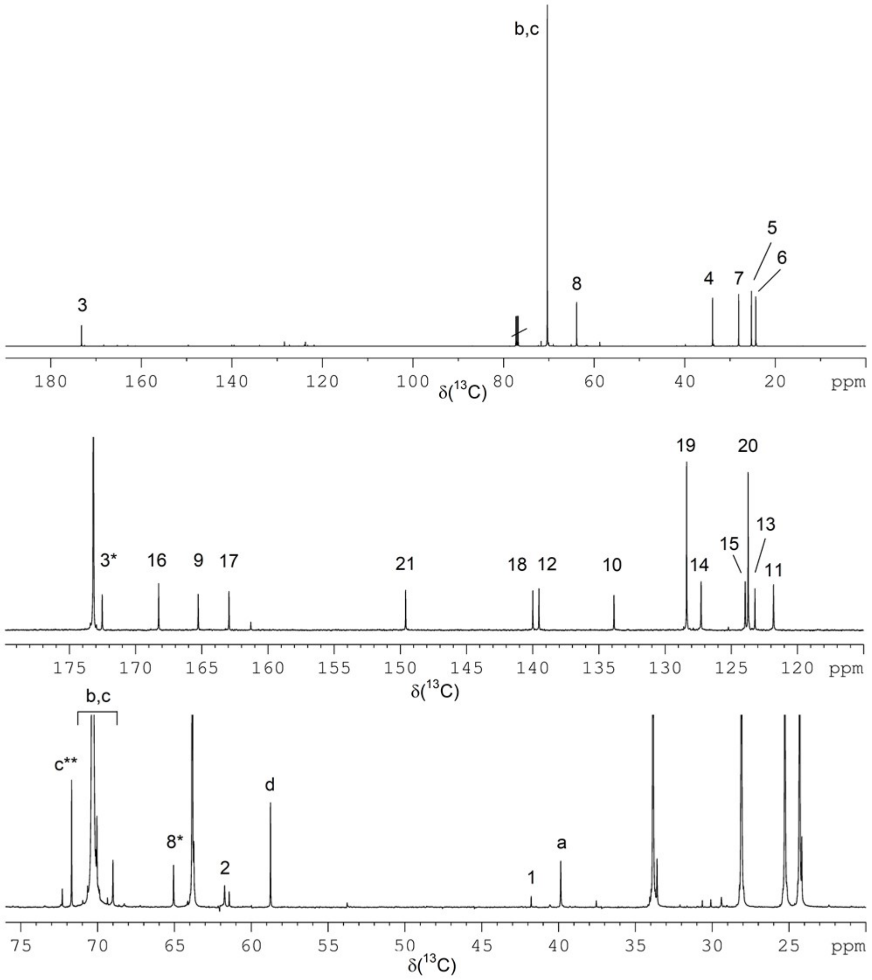

Figure S11. ^{13}C NMR spectrum of **6b** (solvent: $CDCl_3$). Symbol * indicates that the CL unit is bonded to the connecting unit and ** that the EG unit is bonded to connecting unit.

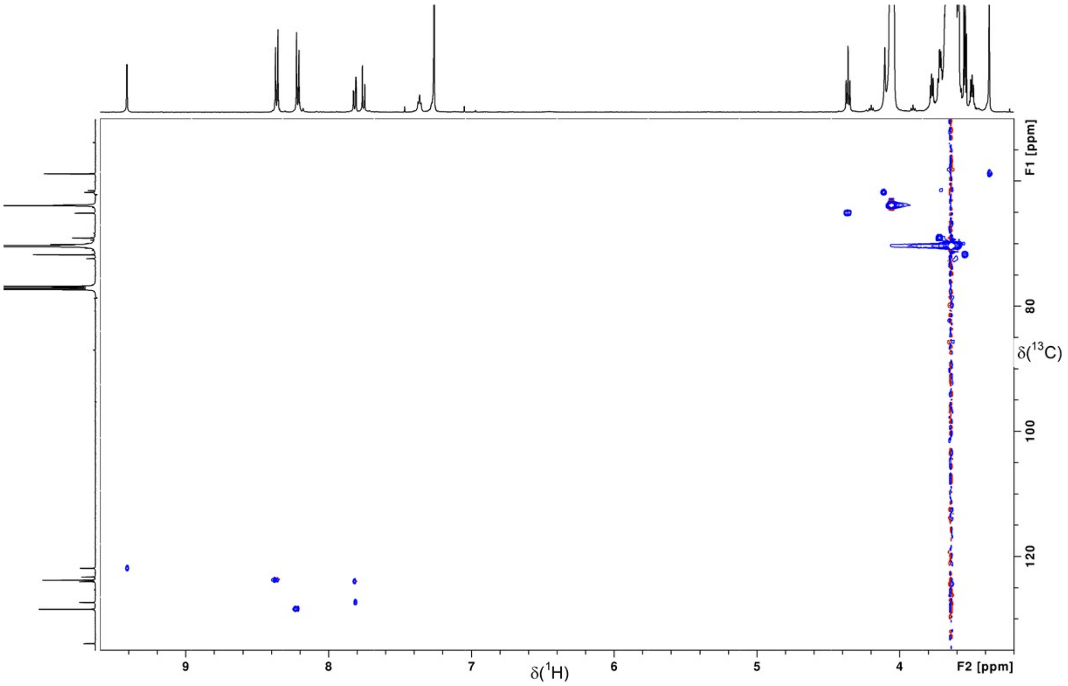

Figure S12. HSQC spectrum (region) of **6b** (solvent: $CDCl_3$).

6. NMR spectroscopic investigation of model compound 7

NMR spectra of partially (A_3B, A_2B_2, AB_3) and completely (B_4) esterified pentaerythrol with dodecanoate as ester moiety.

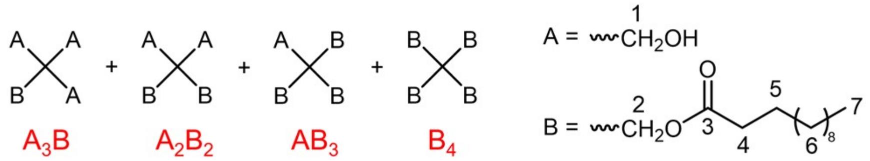

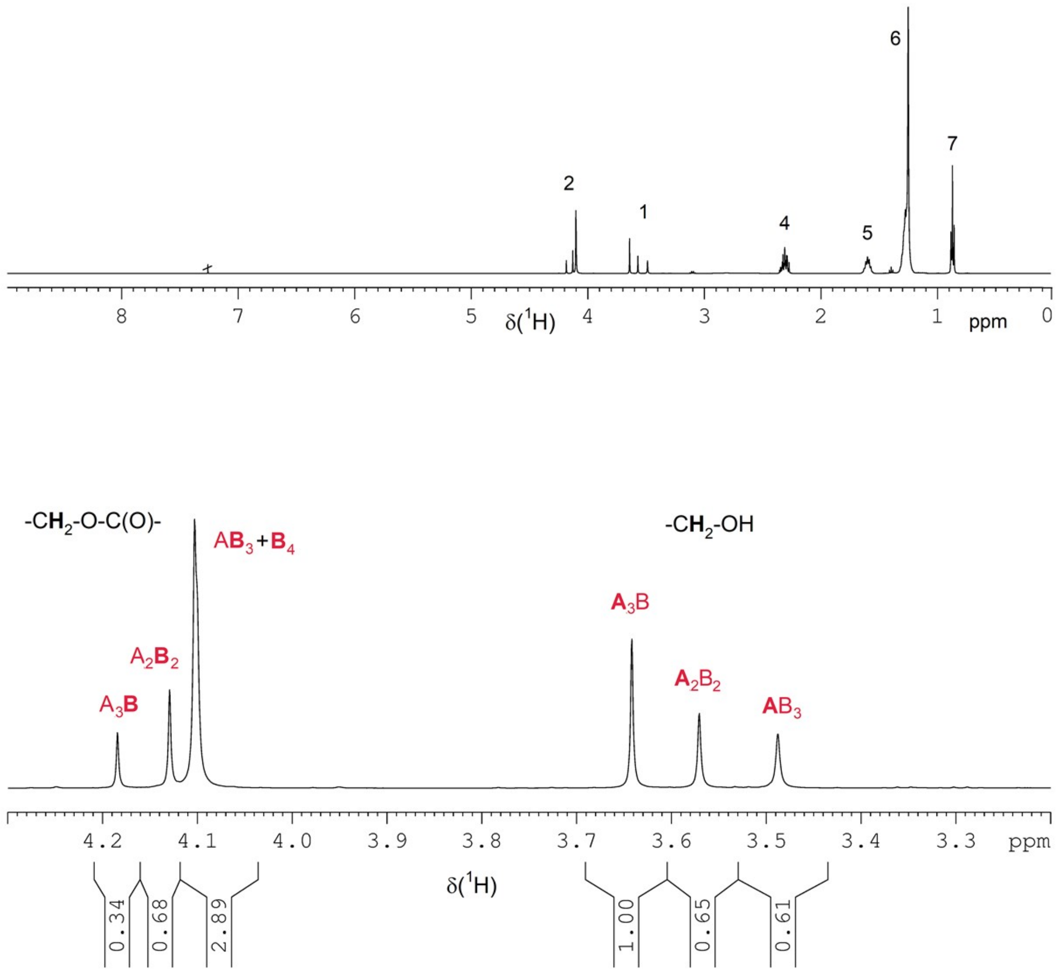

Figure S13. ^{1}H NMR spectrum (top) and enlarged region (bottom) of the mixture of **7** (A_3B – B_4) (solvent: $CDCl_3$).

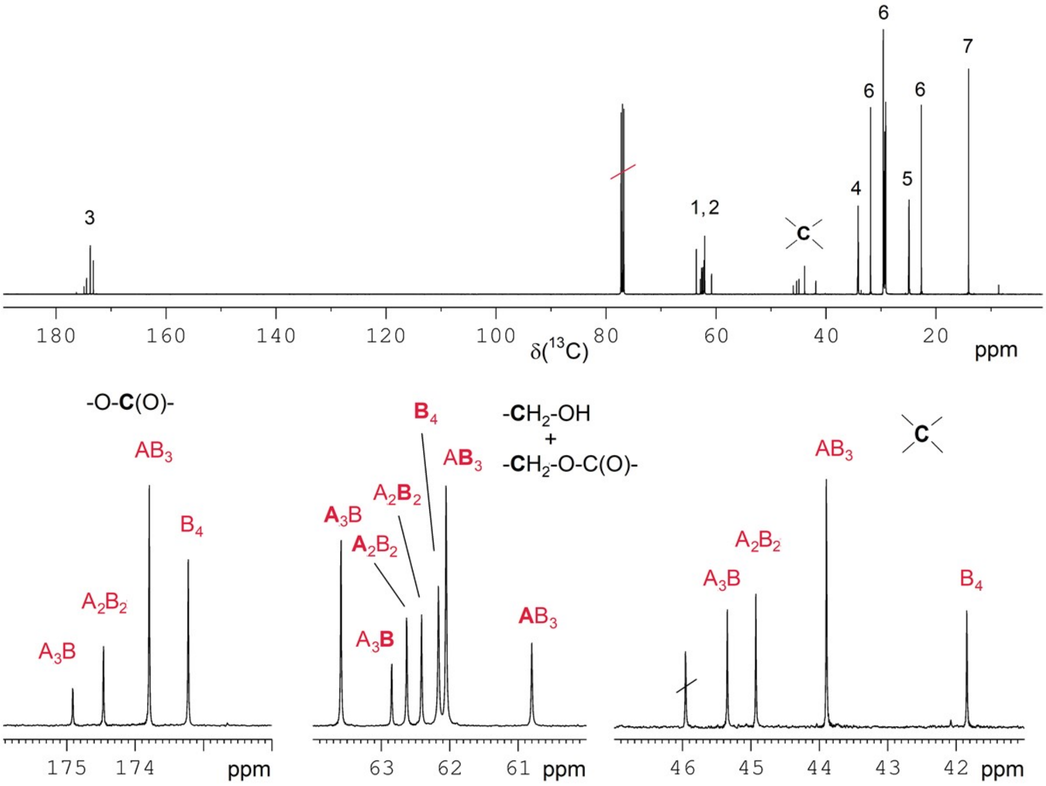

Figure S14. ^{13}C NMR spectrum (top) and enlarged regions (bottom) of the mixture of **7** ($A_3B – B_4$) (solvent: $CDCl_3$).

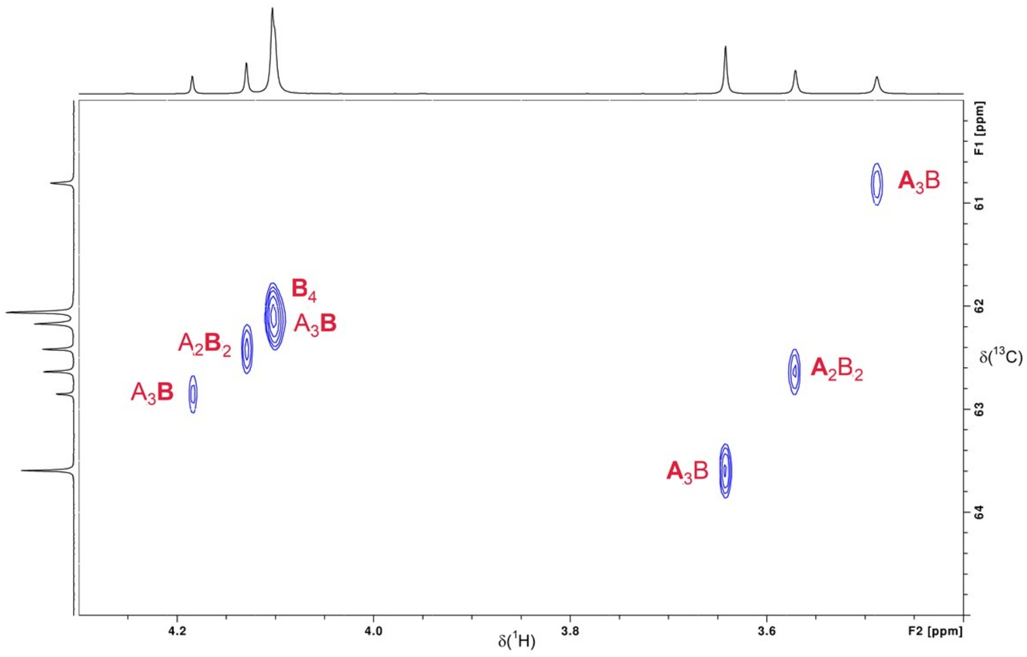

Figure S15. HSQC spectrum (region of $–CH_2OH$ and $–CH_2OR$ groups) of the mixture of **7** ($A_3B – B_4$) (solvent: $CDCl_3$).

7. NMR spectroscopic investigation of model compound 8

NMR spectra of partially (C_3B, C_2B_2, CB_3) and completely (B_4) esterified pentaerythrol with dodecanoate as ester moiety. Initially unreacted hydroxymethylene groups (A) are reacted to benzoxazinone end groups (C).

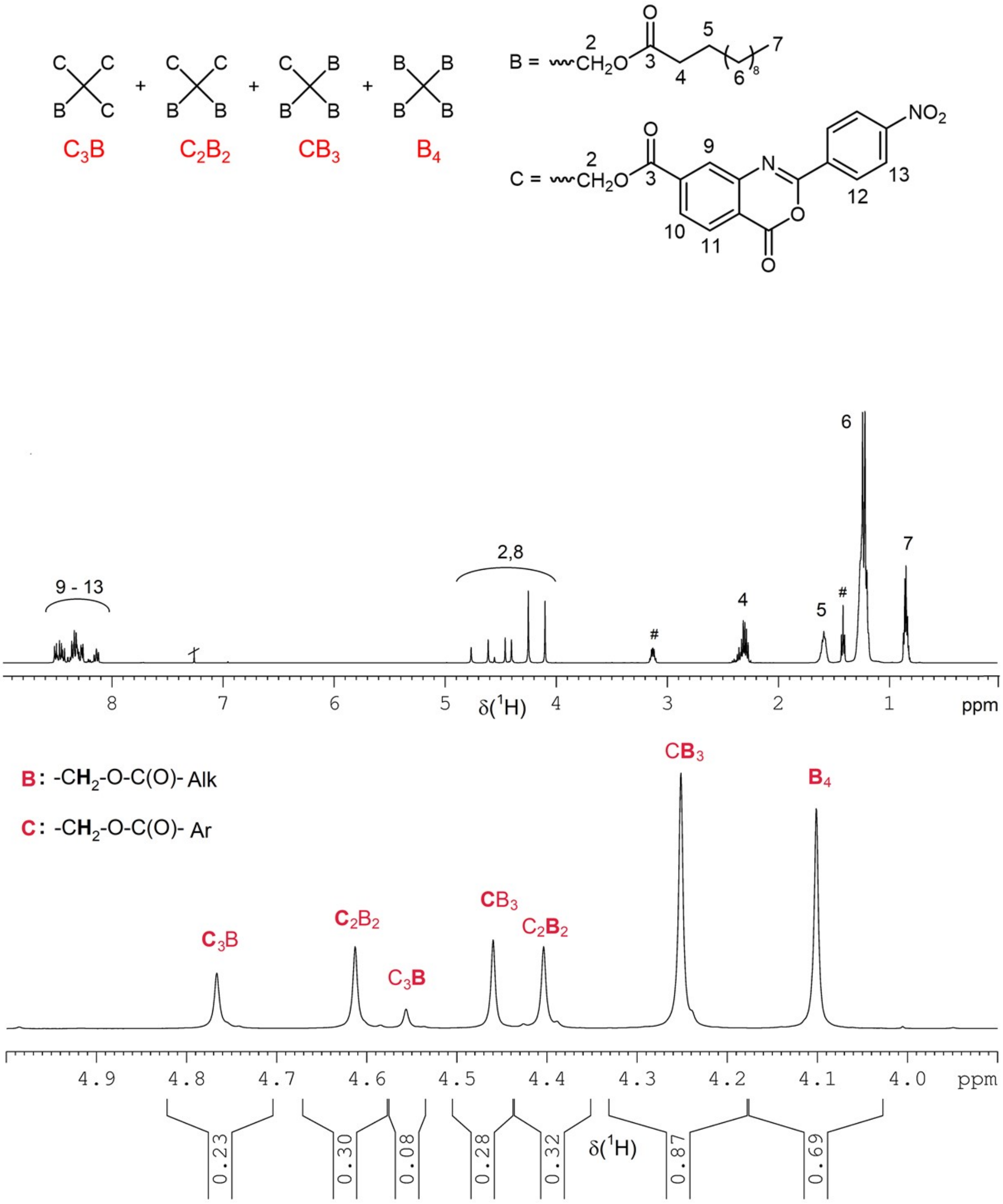

Figure S16. ^1H NMR spectrum (top) and enlarged region (bottom) of the mixture of **8** (C_3B – B_4) (solvent: $CDCl_3$).

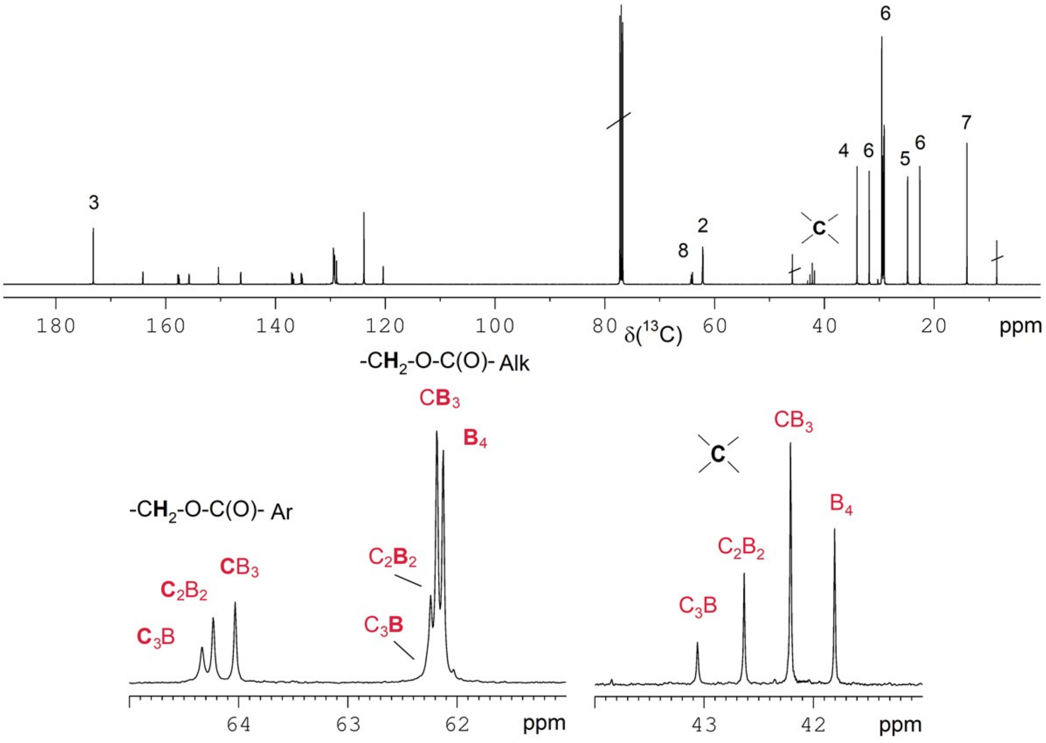

Figure S17. ^{13}C NMR spectrum (top) and enlarged regions (bottom) of the mixture of **8** (C_3B – B_4) (solvent: $CDCl_3$).

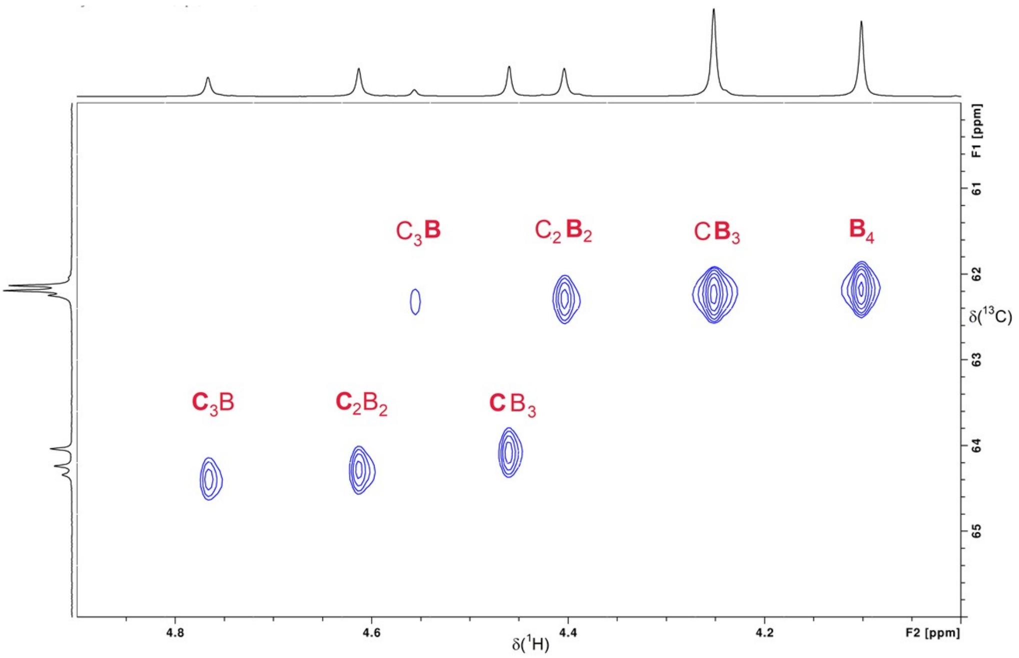

Figure S18. HSQC spectrum (region of –$CH_2OC(O)$Alk and –$CH_2OC(O)$Ar groups) of the mixture of **8** (C_3B – B_4) (solvent: $CDCl_3$).

8. Temperature-dependent ^{1}H NMR spectroscopic investigation of 6a and 6b in water

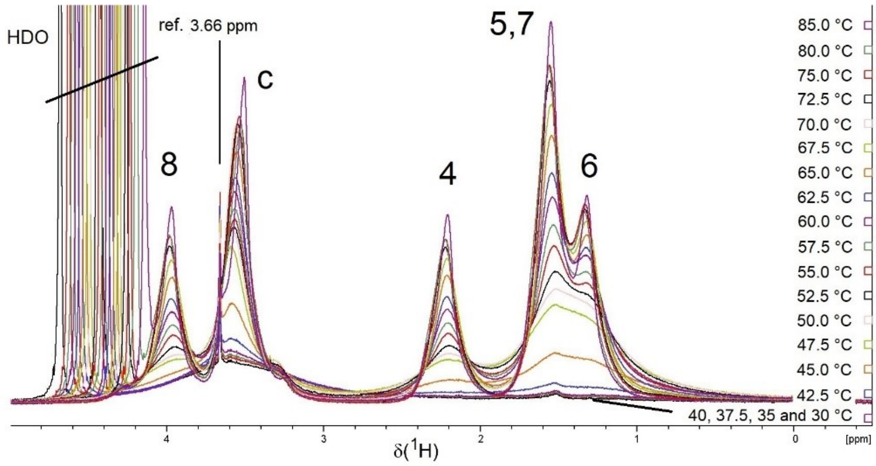

Figure S19a. Variable temperature (VT) ^{1}H NMR spectra (region) of a suspension of **6a** with short PEG chains in D_2O (5 g L^{-1}). The sample is turbid also at 85°C. The signal at 3.66 ppm is a trace of PEG not bonded to the core.

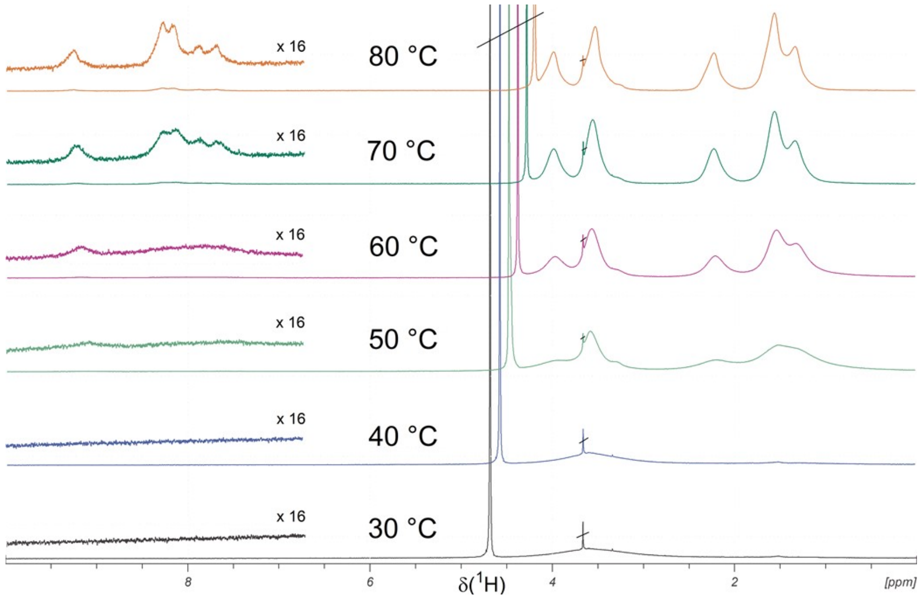

Figure S19b. Selected VT ^{1}H NMR spectra of a suspension of **6a** with short PEG chains in D_2O (5 g L^{-1}). The region of signals of the benzoxazinone-based linking group between PCL star and PEG arms is enlarged by a factor of 16.

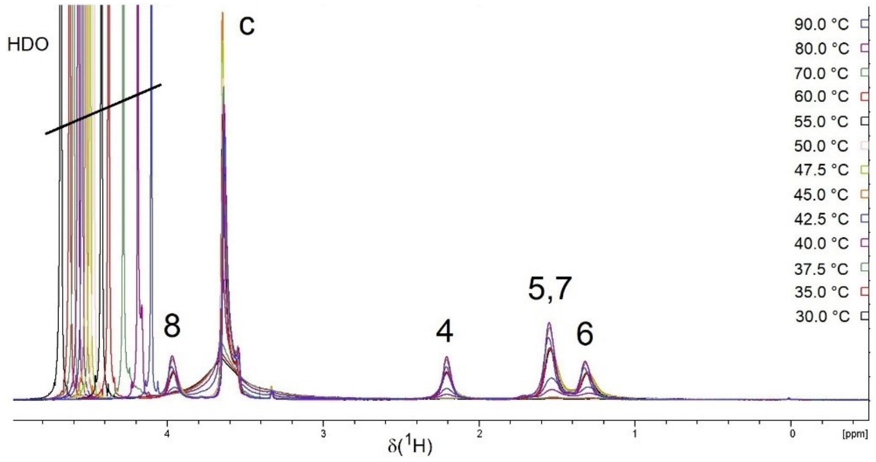

Figure S20a. VT ^{1}H NMR spectra (region) of a suspension of **6b** with long PEG chains in D_2O (5 g L^{-1}). The sample is clear at 90°C and very likely at lower temperatures. The magnification is lower compared to Figure S19a.

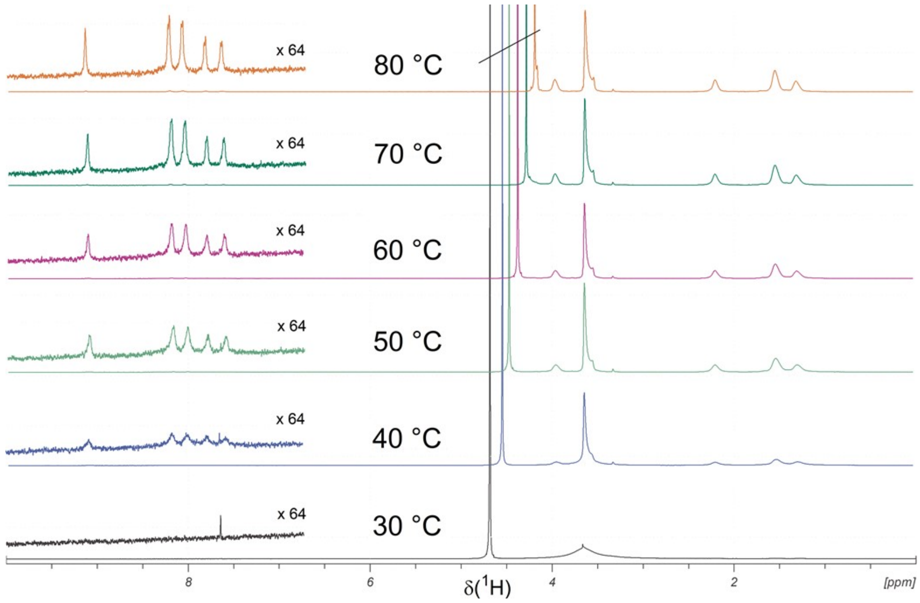

Figure S20b. Selected VT ^{1}H NMR spectra of a suspension of **6b** with long PEG chains in D_2O (5 g L^{-1}). The region of signals of the benzoxazinone-based linking group between PCL star and PEG arms is enlarged by a factor of 64.

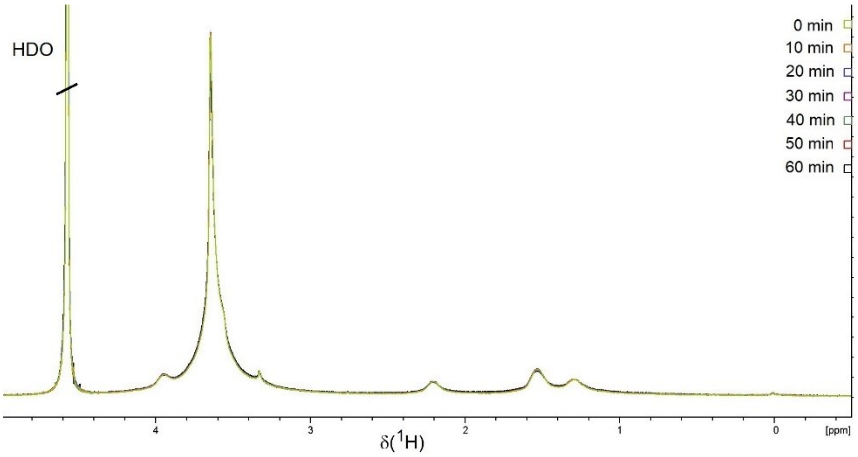

Figure S21. ^{1}H NMR spectra (region) of a suspension of **6b** (long PEG chains) in D_2O (5 g L^{-1}) recorded at 40 °C over a period of one hour. The spectra were recorded during the VT measurements depicted in Figure S20 (heading period).

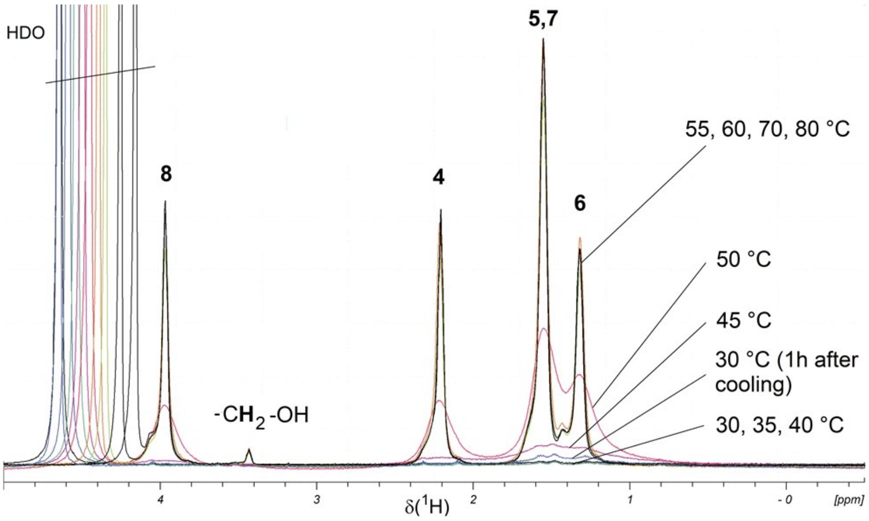

Figure S22. VT ^{1}H NMR spectra (region) of a suspension of **1b** in D_2O (5 g L^{-1}). The sample was turbid over the whole temperature range. Droplets were observed at T > 50°C.

9. Molar mass characterization of 1, 3, 5, 6 by MALDI-TOF and MD-SEC

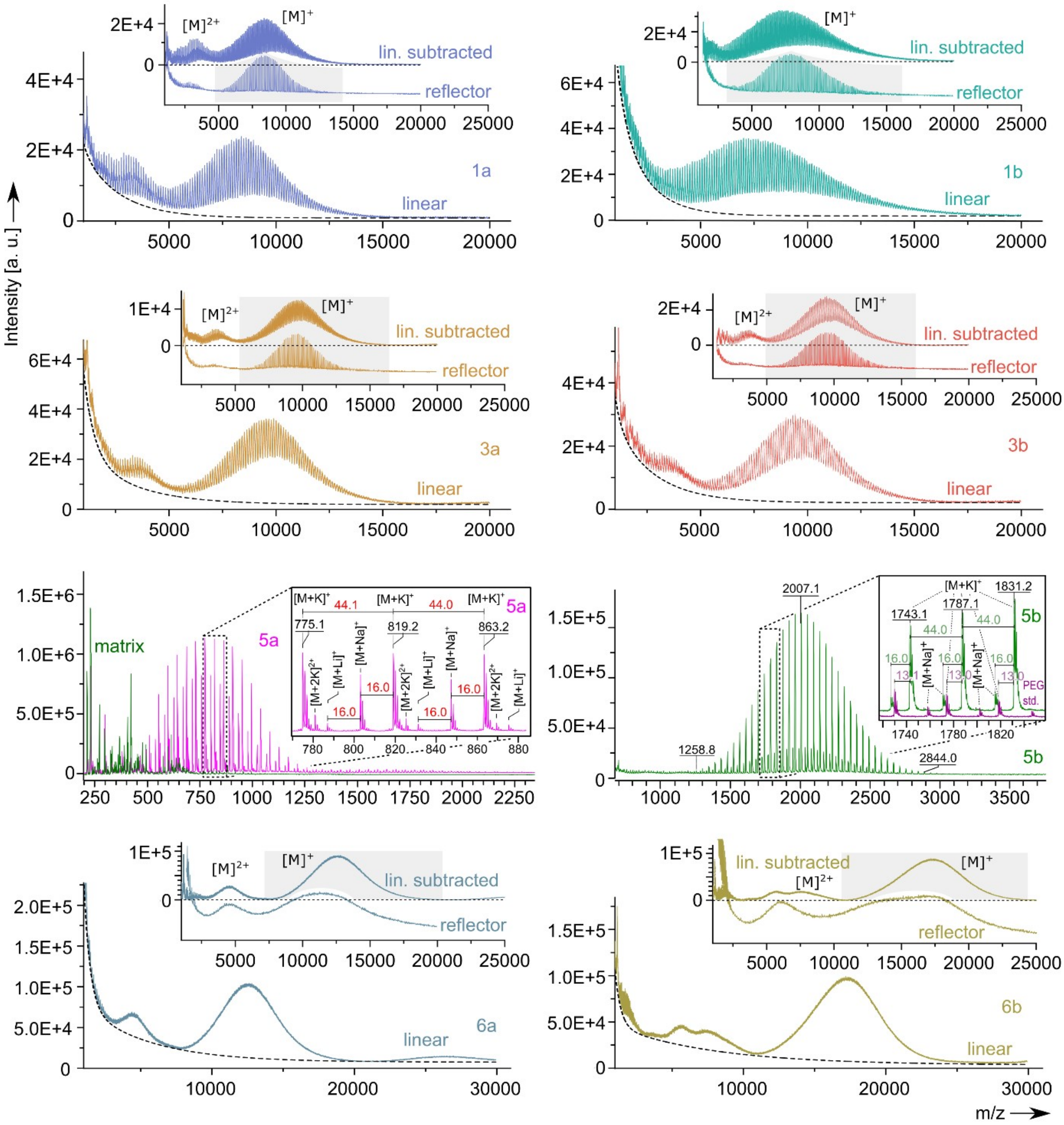

Figure S23. MALDI-TOF MS of **1a, 1b, 3a, 3b, 5a, 5b, 6a** and **6b** measured in linear and reflector TOF mode. For **5a, 5b**, masses below m/z 170 were suppressed by deflection. For all other samples, masses below m/z 700 were suppressed. Spectra of 6000 shots were accumulated each. Calibration and method verification were done with a hydroxy-terminated PEG MALDI-TOF calibration standard (PSS-mixkit) by PSS-Polymer Standards Service GmbH. Spectra recording and evaluation was done by using the software package Compass for flex series, Version 1.4. The dashed lines indicate the baseline being subtracted to yield a baseline-subtracted linear mode spectrum for molar mass average calculation. The molar mass averages reported in Table 1 of the main article were determined from the main fraction (single-charged adduct $[M]^+$) indicated by the marked grey zone. Assignments for 5a, 5b refer to the single-charged main potassium adduct $[M+K]^+$, the sodium adduct $[M+Na]^+$ with Δm/z = -16, the lithium adduct $[M+Li]^+$ with Δm/z = -32 or the double-charged adduct $[M+2K]^{2+}$, respectively.

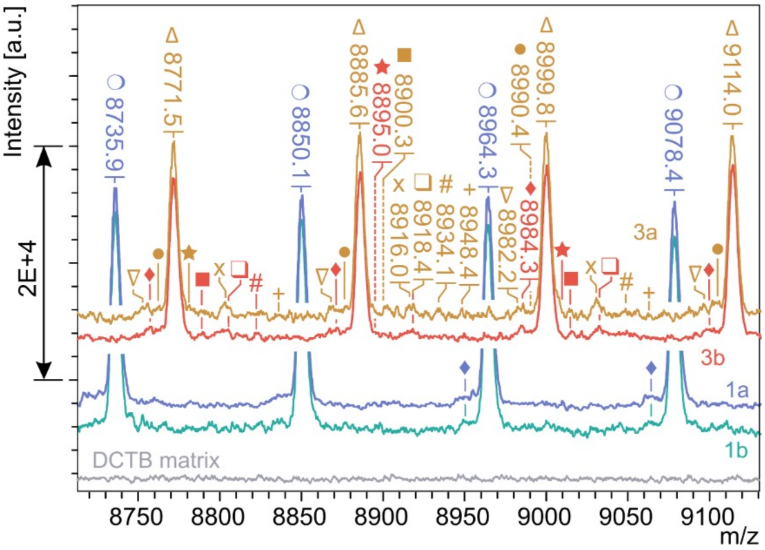

Figure S24. Trace impurity identification in MALDI-TOF mass spectra measured in reflector mode of **1** and **3**. The assigned mass traces are identified as reported in **Table S2**.

Table S2. Identified molecule mass traces found (barely resolved) in the MALDI-TOF mass spectra of **1** and **3**.

Symbol	m/z	m/z$_{theo.}$	Δm/z	Δm/z$_{theo.}$	Matched composition adducts
❍	8964.3	8964.22	-	-	$[P\text{-}(PCL)_{77}H_4 + K]^+$
△	8999.8	8999.68	1177.3	1176.88	$[P\text{-}(PCL)_{67}(Bx\text{-}NO_2)_4 + K]^+$
♦	8984.3	8983.57	1161.4	1160.77	$[P\text{-}(PCL)_{67}(Bx\text{-}NO_2)_4 + Na]^+$
#	8934.1	8933.74	883.1	882.66	$[P\text{-}(PCL)_{69}(Bx\text{-}NO_2)_3H + K]^+$
❑	8918.4	8917.63	867.6	866.55	$[P\text{-}(PCL)_{69}(Bx\text{-}NO_2)_3H + Na]^+$
★	8895.0	8895.65	844.0	844.57	$[P\text{-}(PCL)_{69}(Bx\text{-}NO_2)_3H + H]^+$
▽	8982.2	8981.95	589.0	588.44	$[P\text{-}(PCL)_{72}(Bx\text{-}NO_2)_2H_2 + K]^+$
+	8948.4	8943.86	555.1	550.35	$[P\text{-}(PCL)_{72}(Bx\text{-}NO_2)_2H_2 + H]^+$
×	8916.0	8916.01	294.6	294.22	$[P\text{-}(PCL)_{74}(Bx\text{-}NO_2)H_3 + K]^+$
■	8900.3	8899.91	278.5	278.11	$[P\text{-}(PCL)_{74}(Bx\text{-}NO_2)H_3 + Na]^+$
●	8990.4	8992.07	254.5	256.13	$[P\text{-}(PCL)_{75}(Bx\text{-}NO_2)H_3 + H]^+$
♦	8948.7	8948.11	15.6	16.10	$[P\text{-}(PCL)_{77}H_4 + Na]^+$

Molecule composition declaration:
P- assigns the pentaerythritol core unit
$(PCL)_x$ assigns the no. of poly(ε-caprolactone) repeating units in total
$(Bx\text{-}NO_2)_x$ assigns the no. of 2-(4-nitrophenyl)-benzoxazinone terminal units

Δm/z and Δm/z$_{theo.}$refer to the actual and theoretical mass difference of the identified mass trace to the potassium adduct of a $P\text{-}(PCL)_{xx}H_4$ with equal total number of PCL repeating units.

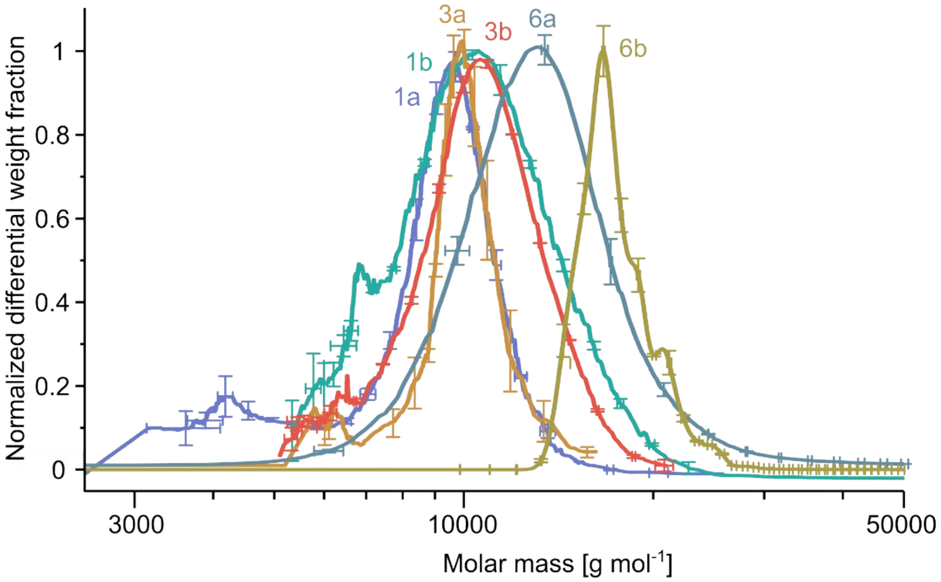

Figure S25. Differential molar mass distribution determined by MD-SEC of the star polymers **1**, **3**, **6a** and **6b** in THF. The corresponding molar mass averages are reported in Table 1 of the main article.

10. Relevant parameters for PCL-b-PEG block and star block copolymers (literature survey)

Table S3. Characteristics of f-arm PCL-b-PEG star block copolymers (references)

Ref.	f a)	Core b)	Tail c)	Strategy d)	M_n e) [10^3 g mol^{-1}]	M_{PCL} f) [10^3 g mol^{-1}]	M_{PEG} f) [10^3 g mol^{-1}]	PDI g)	CMC h)	Size i) [nm]	Type j)
[1]	3, 4	B, P	PEG	**a**	29 - 40	4.7 - 5.1	5 - 5.2	1.17 - 1.32	8 - 22 g L^{-1}	115 - 129	-
[2]	4	C	PEG	**a**	28 - 55	1.9 - 8.6	5	1.23 - 1.34	80 - 322 μg L^{-1}	69 - 71	-
[3]	3, 4	n. i.	PCL	**c**	22 - 31	1.2 - 4.2	5 - 6	1.24 - 1.34	-	20 - 85	-
[4]	4	n. i.	PCL	**c**	24 - 31	1.1 - 2.8	5	1.28 - 1.34	32 - 320 μg L^{-1}	20 - 42	**s**
[5]	3, 4, 8	T, P, n.i.	PCL	**c**	31 - 43	2.6 - 7.3	1.3 - 3.1	1.04 - 1.24	-	-	-
[6]	8	n. i.	PCL	**c**	26 - 29	0.7 - 1.1	2.5	1.22 - 1.23	3 - 4.3 g L^{-1}	20 - 40	-
[7]	4	P	PEG	**c**	11 - 52	0.8 - 8.6	2 - 7.7	1.87 - 2.01	1.1 - 2.1 mg L^{-1}	-	-
[8]	3	T	PEG	**g**	25 - 81	5.1 - 10.3	2 - 4	1.16 - 1.23	1.1 mg L^{-1}	13 - 32	**s**
[9]	4	P	PEG	**g**	27	5.1	2	1.23	10 - 23 mg L^{-1}	45	**s**
[10]	4, 6	P, DP	PEG	**g**	11 - 59	2.3 - 5.5	4.9	1.08 - 1.19	0.43 - 2.1 mg L^{-1}	47 - 361	-
[11]	4→8 k)	P	PEG	**g**	22 - ? l)	1.7	1.1 - 2	1.5 - ?	16 - 79 μg L^{-1}	92 - 105	**s**
[12]	7	β-CD	PEG	**g**	26 - 51	1.2 - 5	1.1 - 2	1.1 ?	-	14 - 42	**s**
[13]	8	R	PEG	**g**	20 - 53 m)	1.5 - 4.5 m)	1 - 2	1.25 - 1.41	0.6 - 2.8 mg L^{-1}	16 - 33	**s**
[14]	16	D	PEG	**g**	131	3.1	5	1.02	3 mg L^{-1}	17/75 n)	-
[15]	32	D	PEG	**g**	215	2.8	5	1.07	-	16/134 n)	**s**

a) Number of star arms

b) Chemical structure of the core: B = 1,3,5-benzenetricarboxylic acid, P = pentaerythritol, DP = dipentaerythritol, C = chlorin, D = polyamidoamine dendrimer, T = tris(hydroxymethyl)propane, β-CD = per-2,3-acetyl-β-cyclodextrin, R = resorcinarene, n. i. = no information

c) Polymer of the outer block

d) Synthesis strategy: **a** = arm first, **c** = core first, **g** = grafting from

e) Number average molar mass of the star

f) Number average molar mass of PCL and PEG blocks (one star arm)

g) polydispersity index of the stars

h) critical micellar concentration in water

i) size of micelles in water

j) type of micelles in water (**s** for spherical micelles)

k) two outer PCL-PEG blocks were attached to each of four inner PCL chains

l) unclear or missing information

m) based on NMR data and PEG precursor weight

n) bidisperse distributions

References for Table S3

[1] K. H. Kim, G. H. Cui, H. J. Lim, J. Huh, C.-H. Ahn, W. H. Jo, *Macromol. Chem. Phys.* **205** (2004) 1684-1692.

[2] C.-L. Peng, J.-J. Shieh, M.-H. Tsai, C.-C. Chang, P.-S. Lai, *Biomaterials* **29** (2008) 3599-3608.

[3] C. Lu, S.-R. Guo, Y-Zhang, M. Yin, *Polym Int.* **55** (2006) 694-700.

[4] C. Lu, L. Liu, S.-R. Guo, Y. Zhang, Z. Li, J. Gu, *Eur. Pol. J.* **43** (2007) 1857-1865.

[5] Y. K. Choi, Y. H. Bae, S. W. Kim, *Macromolecules* **31** (1998) 8766-8774.

[6] S. J. Buwalda, B. Nottelet, J. Coudane, Polymer Degradation and Stability 137 (2017) 173-183.

[7] M. Deng, Y. Chen, L. Piao, X. Zhang, Z. Dai, X. Jing, *J. Pol. Sci A* **42** (2004) 950-959.

[8] G. Jiang, H. Xu, *J. Appl. Pol. Sci.* **118** (2010) 1372-1379.

[9] F. Quaglia, L. Ostacolo, G. Nese, M. Canciello, G. de Rosa, F. Ungaro, R. Palumbo, M. Immacolata La Rotonda, G. Maglio, *J. Biomed. Mater. Res.* **87A** (2008) 563-574.

[10] H. J. Lim, H. Lee, K. H. Kim, J. Huh, C.-H. Ahn, J. W. Kim, *Colloid Polym. Sci.* **291** (2013) 1817-1827.

[11] S. Khoee, A. Kavand, F. H. Nasr, *Polym. Int.* **64** (2015) 1191-1201.

[12] P.-F. Gou, W.-P. Zhu, N. Xu, Z.-Q. Shen, *J. Pol. Sci. A* **46** (2008) 6455-6465.

[13] C. Gao, Y. Wang, W.-P. Zhu, Z.-Q. Shen, *Chin. J. Pol. Sci.* **32** (2014) 1431-1441.

[14] F. Wang, T. K. Bronich, A. V. Kabanov, R. D. Rauh, J. Roovers, *Bioconjugate Chem.* **16** (2005) 397-405.

[15] F. Wang, T. K. Bronich, A. V. Kabanov, R. D. Rauh, J. Roovers, *Bioconjugate Chem.* **19** (2008) 1423-1429.

Table S4. Characteristics of PCL-b-PEG block copolymers (references)

Ref.	Analysis [a]	Type [b]	% PEO [c]	M_n $[10^3$ g mol$^{-1}]$	PDI	Ø [d] [nm]	↔ [e] [nm]
[1]	cryo-TEM	V	0.17 - 0.28	11.4 - 6.8	1.19 - 1.28	100 - 1000+	16 - 18
		C	0.2 - 0.28	9.6 - 5.2	1.2 - 1.28	18 - 21	50 - 1000+
		S	0.34 - 0.43	5.6 - 4.4	1.2 - 1.23	19 - 25	-
[2]	FM, SE	P	≥ 0.11 [h]	13.4 - 20.6	1.48 - 1.57	-	-
		V	0.13 - 0.36	4.1 - 34.6	1.42 - 1.6	~500 - ~5000 [i]	-
		C	0.13 - 0.25	7.9 - 15.5	1.42 - 1.6	-	1000-20000
		S [f]	0.28 - 0.65	1.5 - 19.9	1.23 - 1.6	-	-
[3]	cryo-TEM	C	0.42 - 0.55	≤ 4.77 | ≤ 11.5	≥ 1.19 | ≥ 1.3	11 | 29	10000+
		S	≥ 0.55	≤ 3.9 | ≤ 9.5	> 1.19 | > 1.3	~11 | ~29	-
[4]	FM	V	0.15	14	1.2	100 - 10000	22.5 ± 2.3
[5]	FR, TAN	V	0.09 - 0.25	8 - 21	1.32 - 1.52	60 - 260 [j]	~18 - 36
		S	0.09 - 0.25	8 - 21	1.32 - 1.52	-	-
[6]	TEM with PTA	S	0.15 - 67	4.8 - 32	1-08 - 1.19	10 - 40	-
		C	0.22	8.7	1.05	20	-
		L	0.11 - 0.16	12 - 18	1.09 - 1.10	20	-
[7]	TEM with UAC	S, C, L [g]	0.55	9.1	1.15	22 - 45	-
	cryo-TEM with UAC	C, unclear	0.55	9.1	1.15	24	-

[a] Analysis:
cryo-TEM … TEM of rapidly frozen samples, FM … fluorescence microscopy,
SE … solvent evaporation method, FR … film rehydration method,
UAC … uranyl acetate, TAN… temperature assisted nanoprecipitation,
PTA … phosphotungstic acid.

[b] Types of particles:
S … spherical, C … cylindrical, V … vesicles, L … lamellar structures, P … precipitate.

[c] %PEO is the weight fraction of PEO (virtually identical to volume fraction of PEO) in the polymer.

[d] diameter of the micelles, cylinders, and vesicles.

[e] length of the cylindrical worms or the thickness of the vesicle wall. If cryo-TEM is used, only the dimensions of the PCL core can be analyzed.

[f] S6 of Ref. [2] shows spheres for the smallest polymers, which are not mentioned in Table S1 of Ref. [2].

[g] different morphologies were observed for different concentrations of the stock solution.

[h] calculated using Table S1 of the SI of Ref. [2].

[i] estimated from Figures in Ref. [2] as no quantitative analysis is performed; FR produces vesicles up to 40 μm.

[j] Vesicle diameter increases as a function of the temperature for the TAN method; highest stirring speed and concentrations of 1 mg mL^{-1} were used. Also, a significant dependence on the solvent used for the TAN method is recognized: precipitation from THF produces results comparable to FR, while DMSO, acetone, or methanol produce different results.

References for Table S4

[1] J. A: Zupancich, F. S. Bates, M. A. Hillmyer, *Macromolecules* **39** (2006) 4286-4288.

[2] K. Rajagopal, A. Mahmud, D. A. Christian, J. D. Pajerowski, A. E. X. Brown, S. M. Loverde, D. E. Discher, *Macromolecules* **43** (2010) 9736-9746.

[3] Y. Geng, D. E. Discher, *J. Am. Chem. Soc.* **127** (2005) 12780-12781.

[4] P. P. Ghoroghchian, G. Li, D. H. Levine, K. P. Davis, F. S. Bates, D. A. Hammer, M. J. Therien, *Macromolecules* **39** (2006) 1673-1675.

[5] J. Zhou, R. Ni, Y. Chau, *RSC Advances* **7** (2017) 17997-18000.

[6] Z.-X. Du, J.-T. Xu, Z.-Q. Fan, *Macromolecules* **40** (2007) 7633-7637.

[7] N. Fairley, B. Hoang, C. Allen, *Biomacromolecules* **9** (2008) 2283-2291.

Table S5. Flory-Huggins interaction parameters χ between PEG or PCL and possible good solvents for both polymers (references)

	Ref.	Method a)	T [K]	M_n / M_w [kg mol^{-1}]	Solvents b)					
					THF	TO	AC	CHL	DCM	EA
PEG	[1]	IGC	303	0.4 / -	0.7	-	0.5	-0.4	-0.6	0.8
	[2]	IGC	298 h)	- / 300	-	0.41	0.77	-	-	0.51
	[3]	GLC	343	10.7 / 11.5	-	0.29	-	-0.76	-	-
	[4] c)	GLC	343	4000 / -	0.19	0.39	0.25	-	-	-
	[5]	theory e)	298	- / -	0.38	0.30	0.54	-1.04	-	0.46
	[6]	mixed	373	- / -	0.30	0.26	0.47	-0.55	-0.51	0.39
	[7] d)	IGC	358	35 / -	-	0.769	-	-0.683	-	-
	[8]	swelling	298	4.6 / 5.2	0.38	-	0.451	-	-	-
	[9]	viscosity f)	298	11.4 / 12.4	0.41	0.38	-	-1.61	-	-
PCL	[5]	theory e)	298	- / -	0.18	0.09	0.64	-0.71	-	0.36
	[6]	mixed	373	- / -	0.13	0.08	0.46	-0.4	-0.26	0.36
	[9]	viscosity f)	298	10.4 / 10.6	-0.05	0.07	-	-0.54	-	-
	[10]	IGC	343	33 / -	-	-0.01	-	-	-	0.32
	[11]	IGC	343	33 / -	0.30	-	-	-	-	-
	[12]	IGC	343	- / -	0.13	0.06	0.55	-0.6	-	0.36
	[13]	visual g)	298	14, 65 / -	s-p i)	s-n j)	p-n k)	s	-	p-n k)

a) Inverse gas chromatography (IGC), gas-liquid chromatography (GLC), swelling refers to an analysis where the Flory-Rehner and Bray-Merill model were enriched by a discussion of network defects [14].

b) Tetrahydrofuran (THF), toluene (TO), acetone (AC), chloroform (CHL), dichloromethane (DCM), ethyl acetate (EA).

c) Original data were re-analyzed by Monique Galin and taken from Table 2 of Ref. [4].

d) Only data for 10K PEG at lowest temperature is included in the table.

e) theoretical estimate based upon the model of Tian and Munk [6]; parts of these data were published previously [13].

f) viscosity data for ~11K star polymers was normalized by an average over the corresponding interaction estimates of Ref. [6] for PEG and PCL and refers to the dilute limit.

g) PEG with 14K and 65K molar mass was dissolved in rather high concentrations (either 0.5 g or 2.5 g per 5 ml of solvent) and the solution was checked visually regarding dissolution of the polymer. The results were classified as soluble (s), partially soluble (p), and non-soluble (n).

h) extrapolated from temperature range 343-363 K.

i) 65K PEG at large concentrations was only partially soluble.

j) 14K PEG was soluble, while 65K was partially soluble at low concentrations and non-soluble at high concentrations.

k) 14K PEG was soluble, while 65K was not.

The interactions between PEG or PCL and the potential good solvents tetrahydrofuran (THF), toluene (TO) acetone (AC), chloroform (CHL), dichloromethane (DCM), and ethyl acetate (EA), were analyzed in several works based upon different methods, see Table. The scatter of the data stems in part from the method since the interaction parameters depend on polymer volume fraction [14] and measurement temperature T [15] (chromatographic data refers to the limit of high polymer volume fractions, swelling data is obtained in the semi-dilute regime, while viscosity data is collected in the dilute limit). End group corrections [16] were minimized by selecting the data for the largest polymers and temperature dependence was reduced by selecting measurement conditions closest to room temperature, if possible. Altogether, chloroform and dichloromethane are very good solvents for both polymers independent of the concentration range for all temperatures under investigation. THF and toluene are good solvents for PCL but may cross-over to theta or poor for PEG depending on experimental conditions. Ethyl acetate has somewhat poorer solvent quality than these for both polymers, while acetone is theta to poor for both polymers.

References for Table S5

[1] F. Sesigur, D. S. Dasdan, O. Yazici, F. Cakar, O. Cankurtaran, F. Karaman, *Optoelectr. Adv. Mater. Rapid Commun.* **10** (2016) 97-101.

[2] M.J. Fernandez-Berridi, T.F. Otero, G.M. Guzman, J.M. Elorza, *Polymer* **23** (1982) 1361-1366.

[3] M. Galin, *Polymer* **24** (1983) 865-870.

[4] Y. H. Chang, D. C. Bonner, *J. Appl. Polym. Sci.* **19** (1975) 2439.

[5] M. Tian, P. Munk, *J. Solution Chemistry* **24** (1995) 267-284.

[6] J. E. Mark, Physical Properties of Polymers, Handbook, Springer Verlag(2006).

[7] K. Adamska, A. Voelkel, *Journal of Chromatography A* **1132** (2006) 260-267.

[8] N. J. Rebello, H. K. Beech, B. D. Olsen, *ACS Macro Letters* **10** (2021) 531-537.

[9] C. Bunk, L. Löser, N. Fribiczer, H. Komber, L. Jackisch, R. Scholz, B. Voit, S. Seiffert, K. Saalwächter, M. Lang, F. Böhme, *Macromolecules* **55** (2022) 6573-6589.

[10] A. Sarac, D. Sakar. O. Cankurtaran, F. Y. Karaman, *Polymer Bull.* **53** (2005) 349-357.

[11] A. Sarac, Ö. Cankurtaran, F. Yilmaz, *Macromol. Symp.* **217** (2004) 301-306.

[12] M. Tian, P. Munk, *J. Chem. Eng. Data* **39** (1994) 742-755.

[13] C. Bordes, V. Freville, E. Ruffin, P. Marote, J. Y. Gauvrit, S. Briancon, P. Lanteri, *Int. J. Pharmaceutics* **383** (2010) 236-243.

[14] N. Schuld, B. A. Wolf in *Polymer Handbook*, Eds. J. Brandrup, E. H. Immergut, E. A. Grulke, 4th Edition, Wiley, New York (2003), Chapter VII pp 247-264.

[15] C. M. Hansen, *Hansen Solubility Parameters*, A User's Handbook, 2nd edition, Taylor & Francis Group, LLC (2007).

[16] J. Klein, H. E. Jeberien, *Makromol. Chem.* **181** (1980) 1237.